

## A Disposable Electrochemical Immunosensor Based on PDDA-functionalized Graphene/Gold Nanoparticles Composites for Detection of Inflammatory Cytokine Interleukin-22

Yuqi Yan<sup>1</sup>, Shanshan Shi<sup>1</sup>, Jiuyang Yu<sup>4</sup>, Mengyuan Zhang<sup>1</sup>, Yaru Zhang<sup>2</sup>, Hongxin Huang<sup>1</sup>, Jiong Li<sup>3</sup>, Zhenyou Jiang<sup>1,\*</sup>

<sup>1</sup> Department of Microbiology and Immunology, Jinan University, Guangzhou 510632, People's Republic of China; Guangdong Key Laboratory of Molecular Immunology and Antibody Engineering, Jinan University, Guangzhou 510632, People's Republic of China.

<sup>2</sup> Department of Chemistry, Jinan University, Guangzhou 510632, People's Republic of China

<sup>3</sup> Department of Anatomy, Jinan University, Guangzhou 510632, People's Republic of China

<sup>4</sup> Department of Microbiology and Biochemical pharmacy, Jinan University, Guangzhou 510632, People's Republic of China

\*E-mail: [tjzhy@jnu.edu.cn](mailto:tjzhy@jnu.edu.cn)

Received: 5 May 2015 / Accepted: 8 June 2015 / Published: 24 June 2015

---

A sandwich-format electrochemical immunoassay strategy was proposed for the single-protein detection of inflammatory cytokine, Interleukin-22 (IL-22). The capture anti-IL22 (Ab<sub>1</sub>) and detection anti-IL22 (Ab<sub>2</sub>) were immobilized onto poly(dimethyldiallylammonium chloride)-functionalized graphene/gold nanoparticles nanocomposites (PDDA-G/AuNPs) modified indium tin oxide-coated glass (ITO) electrodes. When the immunosensor was incubated with sample antigens and biotin-modified Ab<sub>2</sub> successively, streptavidin-modified horseradish peroxidase (HRP) was immobilized to produce the electrochemical signal by using o-phenylenediamine (OPD) and H<sub>2</sub>O<sub>2</sub> as the electrochemical substrates. The linear ranges of IL-22 were from 5 to 5000 pg mL<sup>-1</sup> with the detection limits of 0.5 pg mL<sup>-1</sup> (S/N=3), which is lower than that of the conventional ELISA. Experimental results demonstrated a ultrasensitive proposed immunosensor and revealed a selective and reproducible measurement of bioactive molecules in clinical diagnosis and therapy.

---

**Keywords:** Graphene, Interleukin-22, Immunosensor, Electrochemical detection

### 1. INTRODUCTION

Interleukin-22 (IL-22) produced by many different types of lymphocytes, a member of the IL-10-like cytokine family, plays a critical role in inflammation, tissue protection, regeneration and

antimicrobial defence[1-3]. IL-22 has been involved in several autoimmune diseases such as systemic lupus erythematosus (SLE), rheumatoid arthritis (RA), multiple sclerosis (MS), Sjogren's syndrome (SS) and graft versus host disease (GHVD)[4-5]. IL-22 is also associated with human skin diseases[6], anti-tumor immunity[7], maintaining barrier homeostasis against intestinal pathogens and commensal bacteria[8]. Therefore, detecting the presence of IL-22 in physiological may have great significances for both diagnostics and therapeutics potential.

Compared with traditional detection methods, electrochemical immunoassay is considered to as an ideal strategy among various measurement techniques for biomarkers because of its portability, low cost and high sensitivity, especially in resource-limited conditions[9-10]. The biologically active materials are crucial to electrochemical sensors, in which the enzymes have been widely used on account of high selectivity and catalytic activity. These enzymes can be fixed on the sensor surface to form an enzyme-sensitive film either by physical methods such as adsorption and embedding, or by chemical linking methods[11]. After that, the electrode is used as a chemical signal converter to determine the electron transfer produced by the enzyme catalysis of a particular target substance. Thereby, the concentration of the target substance is indirectly measured by electrochemical sensors. ITO electrode, a sheet of glass coated Indium tin oxide ,is one of the most attractive photoelectric material due to their outstanding performance of high light permeability and satisfactory electrical conductivity[12]. ITO electrode exhibits superior performance than other conventional with low resistivity , easily engraving, resistance to wear chemical corrosion, Inexpensive price, large-scale use and so on.Numerous studies have been reported on the sensing applications of ITO electrodes such as immunosensor platform[13], direct determination of cell viability[14], highly sensitive virus sensor[15], electrochemical hormone biosensors[16] and microfluidic device for real-time detection[17]. Therefore,these properties have pointed the extensive applications of ITO as a disposable electrodes for electrochemical biosensor.

Graphene, which can be warped into zero-dimensional fullerenes or curled to three-dimensional carbon nanotubes, is the basic units of other graphite materials.) Generally, graphene sheets can be easily synthesized from chemical reduction of exfoliated graphene oxide in low cost[18]. The excessive residual defects and oxygenated functional groups in graphene , however, have a bad effect on its electronic and electrocatalytic performances[19]. To effectively eliminate the defects and oxygen contents in graphene, poly(diallyldimethylammonium chloride) (PDDA), a positively charged polyelectrolyte, has been used to prepare graphene from exfoliated GO[20] and[21] PDDA-functionalized graphene (PDDA-G) can avoid undesirable reactions and has a higher electron transfer kinetics and excellent catalytic activity to modify electrode. Gold nanoparticles (AuNPs) are extensively used in analytical research due to simply controllable preparation process, uniform particle sizes, biocompatibility, surface reactivity, high catalytic efficiency and stable performance[22-23]. Owing to good biocompatible, AuNPs can be incorporated directly with biological molecules by affinity biosensing or covalent interactions without affecting the immobilized proteins activity to constitute biological probe conjugate. In addition, their large surface area greatly enhance the biomolecular load. AuNPs can promote electron transport between the active site of the enzyme and the microenvironment in the reaction system. As collaborative results of PDDA-G/AuNPs nanocomposites,it is possible to improve the current response of the sensor effectively.

In this work, we reported a facile and green approach to PDDA-G/ AuNPs nanocomposites and a sandwich-type (Scheme 1c) electrochemical immunosensor which OPD and  $\text{H}_2\text{O}_2$  were used as substrate for detection of IL-22. After reduction, the PDDA-G could highly accelerate electron transfer and amplify electrochemical signal effectively. Further modification of PDDA-G with AuNPs could enhance capture antibodies loading and signal generation on the surface of ITO electrodes. The as-prepared PDDA-G/AuNPs/ITO sensor showed excellent electrocatalytic properties against IL-22. Also, owing to the stable electrochemical properties and its low cost, the transparent electrode had been widely used in the field of electrochemistry. This sensor offered several advantages such as wide linear working ranges, low limit detection, and made its high value in bio-sensing fields.

## 2. EXPERIMENTAL

### 2.1 Reagents and materials

Interleukin-22 (IL-22) standard solutions, monoclonal antihuman IL-22 capture antibodies ( $\text{Ab}_1$ ), biotinylated antihuman IL-22 detection antibodies ( $\text{Ab}_2$ ), and streptavidin–HRP were purchased from Linc-Bio Company (China). Hydrogen tetrachloroaurate hydrate ( $\text{HAuCl}_4 \cdot x\text{H}_2\text{O}$ , 99.9%) was purchased from Alfa Aesar (China). Sodium borohydride ( $\text{NaBH}_4$ ) were purchased from Sigma-Aldrich (USA). Poly dimethyl diallyl ammonium chloride (PDDA) was obtained from TCI (Japan). Graphene oxide was purchased from JCNANO (China).  $\text{NaH}_2\text{PO}_4$ ,  $\text{Na}_2\text{HPO}_4$ ,  $\text{NaOH}$ ,  $\text{H}_3\text{PO}_4$ ,  $\text{K}_4\text{Fe}(\text{CN})_6$ ,  $\text{K}_3\text{Fe}(\text{CN})_6$ , Tween 20, bovine serum albumin (5% BSA) and o-phenylenediamine (OPD) were purchased from Shanghai Chemical Reagents Company (China). Clinical serum samples were provided by the First Affiliated Hospital of Jinan University, China. All solutions were prepared with ultrapure water (resistivity  $>18 \text{ M}\Omega$ ) throughout the experiment. Indium tin oxide (ITO) sheets (resistance  $15 \Omega \text{ cm}^{-1}$ ) were purchased from Shenzhen YH Company (China). Other reagents were of analytical grade and used as received.

### 2.2 Apparatus

Transmission electron microscopy (TEM) images were taken from a JEOL-100CX electron microscope (H7650, Hitachi, Japan). X-Ray Diffraction (XRD) analysis was recorded on a D/max2550VB X-ray diffractometer (Rigaku, Japan). All electrochemical experiments were measured on a CHI660 electrochemical workstation (Shanghai Chenhua Instrument, China) with a three-electrode system composed of a platinum wire as auxiliary electrode, a saturated calomel as reference electrode (SCE) and the modified ITO electrode as working electrode. Cyclic voltammetry (CV) measurements were carried out in  $5 \text{ mM Fe}(\text{CN})_6^{3-/4-}$  with  $0.1 \text{ M KCl}$ , and the differential pulse voltammetry (DPV) measurements were carried out in  $0.1 \text{ M}$  phosphate-buffer saline (PBS) containing different concentrations of OPD and  $\text{H}_2\text{O}_2$  with various pH at room temperature.

### 2.3 Preparation of PDDA-functionalized graphene

Graphene oxide(GO) was obtained from the precursor of graphite powder by modified Hummer method[24]. Then,PDDA-functionalized graphene (PDDA-G) was synthesized following the previous protocol with a slight modification[25]. To start with, 50 mL GO ( $1 \text{ mg mL}^{-1}$ ) was sonicated for 30 h. Secondly, 1 mL PDDA ( 20% ) was added into the homogeneous GO dispersion, and then the solution was sonicated for another 30 min. Subsequently, this solution was being continuously heated for 2 min following a 2-min rest by a household microwave oven (power: 600 W) for 10 min. After several washings and centrifugations(at 10,000 rpm for 20 min), the collected product was redispersed completely in water/ethanol mixture for further use. To prepare PDDA-GN through a microwave-assisted heating procedure , PDDA was both used as a reducing reagent and stabilizer[26].

### 2.4 Preparation of AuNPs

The AuNPs used in this work were synthesized according to a reported reference[27]. To prepare AuNPs, 3 mL sodium citrate solution (1%) was added into 100 mL boiling  $\text{HAuCl}_4$  solution(0.01%) with vigorous stirring. After continuously boiling for 15 min and cooling off at room temperature, the obtained red wine nano gold solution then was poured in  $4^\circ\text{C}$  refrigerator for storage spare.All steps were performed at room temperature unless otherwise stated.

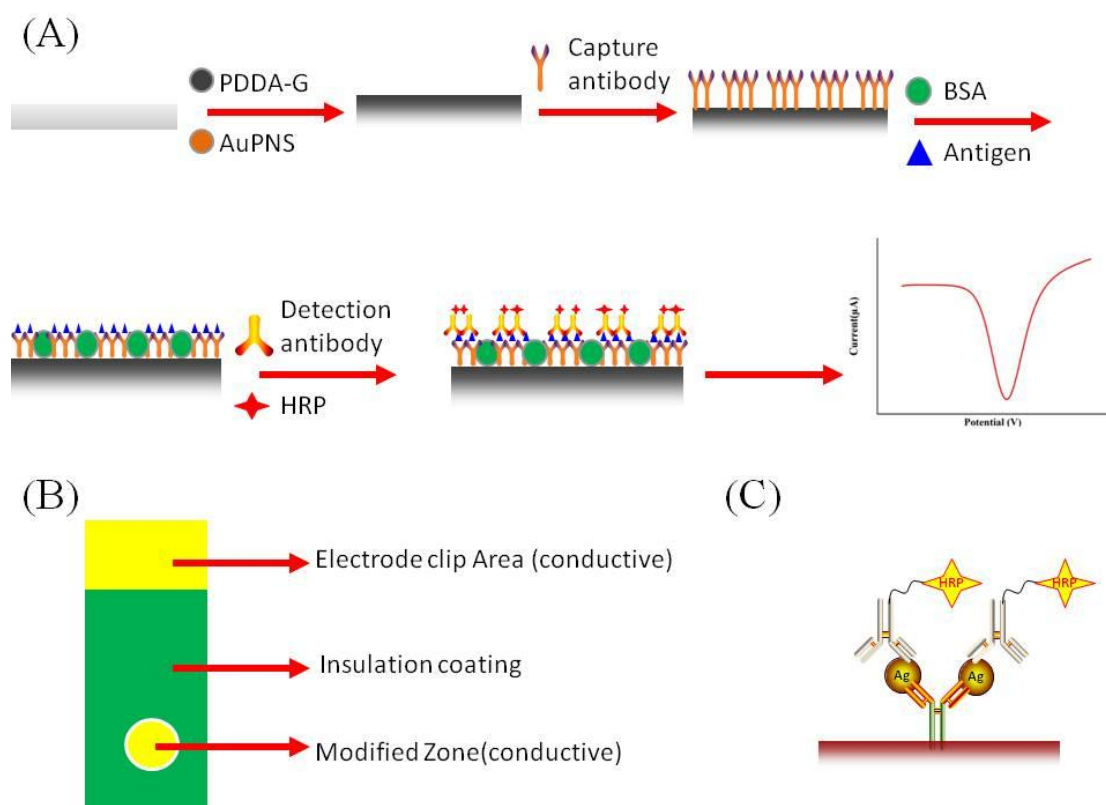
### 2.5 Fabrication of the PDDA-G/AuNPs /ITO immunosensor

A piece of ITO sheet was cut into  $1.5 \text{ cm} \times 2.0 \text{ cm}$  slides and sonicated successively in ethanol (10 min) and deionized water ( 5 min ),and then dried by pure nitrogen.Next, Nail enamel (epoxy resin) was cast onto the ITO slide with an exposed surface area of  $0.126 \pm 0.002 \text{ cm}^2$  as a Working electrode (WE), while leaving the upper area for electrical connection according to a reference[28] ( Scheme 1b). Then, 10  $\mu\text{L}$  as-prepared PDDA-G solution was cast fully covering the exposed ITO surface and dried under ambient temperature. Gold nanoparticles (AuNPs) was assembled onto the electrode, followed by another washing with PBS (0.1 M, pH 7.3).Then the obtained ITO electrodes were incubated with 10  $\mu\text{L}$   $25 \mu\text{g mL}^{-1}$  antihuman IL-22 capture antibodies( designated as  $\text{Ab}_1$  ) solution at  $4^\circ\text{C}$  overnight. Subsequently, excess antibodies and loosely binding chemicals were thoroughly eliminated with Tween-20 (0.05% in PBS buffer) and PBS buffer (0.1 M, pH 7.3) for 3 minutes each, and then 10  $\mu\text{L}$  BSA ( 5% ) was employed to block possible remaining active sites and minimize the non-specific adsorption for 1 h at  $37^\circ\text{C}$ .

### 2.6 Measurement procedure

The sensor was carefully incubated with the IL-22 standard solutions or serum samples with various concentrations for 35 min at  $37^\circ\text{C}$  on the area of modified ITO, and then it was treated with

the biotinylated antihuman IL-22 detection antibodies (designated as Ab<sub>2</sub>) to immunoconjugate for 30 min at 37 °C, followed by streptavidin-modified HRP for 30 min at 37 °C resulting in forming the amplified system of HRP–Ab<sub>2</sub>. After every step, the electrode was cleaned with Tween-20 (0.05% in PBS buffer) and PBS buffer (0.1 M, pH 7.3) for 3 minutes respectively. Subsequently, The immunosensor was placed in an electrochemical cell containing 10 mL PBS buffer (pH 6.5) with OPD (0.2mM) and H<sub>2</sub>O<sub>2</sub> (0.1 mM) as mediators to produce the electrochemical signal. DPV was then used from –0.2 V to 0.6 V with a frequency of 15 Hz and a pulse amplitude of 25 mV. Besides, the fabrication process of the sandwich immunosensor is illustrated in Scheme 1a.



**Scheme 1** a Schematic illustration of the sandwich electrochemical immunodetection protocol. b Design of the ITO electrode. c Typical graph of a sandwich immunoassay

### 3. RESULTS AND DISCUSSION

#### 3.1 Characterization of the PDDA-G/AuNPs /ITO

In the view of its unique properties, PDDA-G is expected to serve as the "linker arm" among bio-sensitive materials and the transducer to construct an ideal biosensor platform. The TEM images of the GO and PDDA-G (Fig. 1a and b) were employed to show their characteristic wrinkled and corrugated sheet structure. After microwave-assisted reduction, PDDA-G was overlapped in the form of flake-like nanostructures, folded and plicated into intermittent crumpled sheet structures, which

could greatly increase the surface roughness and area[29]. Moreover, the morphology of AuNPs was further observed by TEM(Fig. 1c), which showed that AuNPs were evenly distributed in the ITO.

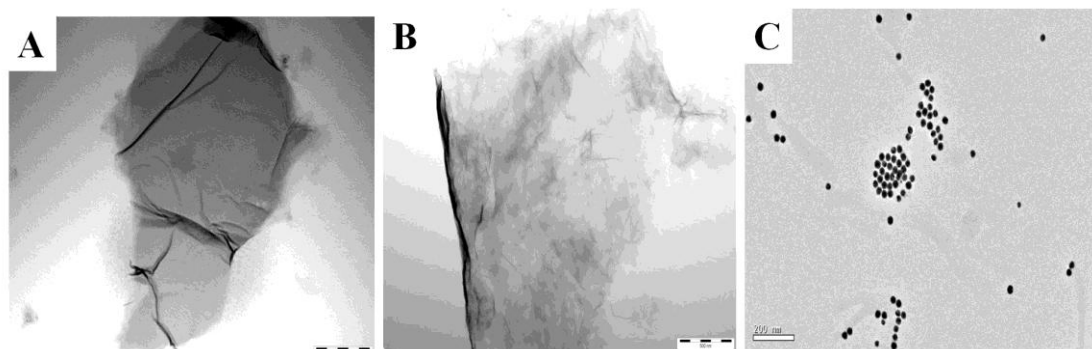


**Figure 1.** TEM images of **a** graphene oxide, **b** PDDA-G nanocomposites, **c** AuNPs

The as-prepared PDDA-G was further characterized by UV and X Ray Diffraction. Fig. 2a shows UV-vis spectra of GO(curve a), PDDA-G (curve b). Markedly, there are two obvious UV absorption peaks at 230 nm in GO(curve a) and 260 nm in PDDA-G nanocomposites (curve b). The peak at 260 nm is the result of the electronic conjugation in PDDA-G nanosheets[30], which indicated the successful reduction procedure of PDDA-G nanosheets.

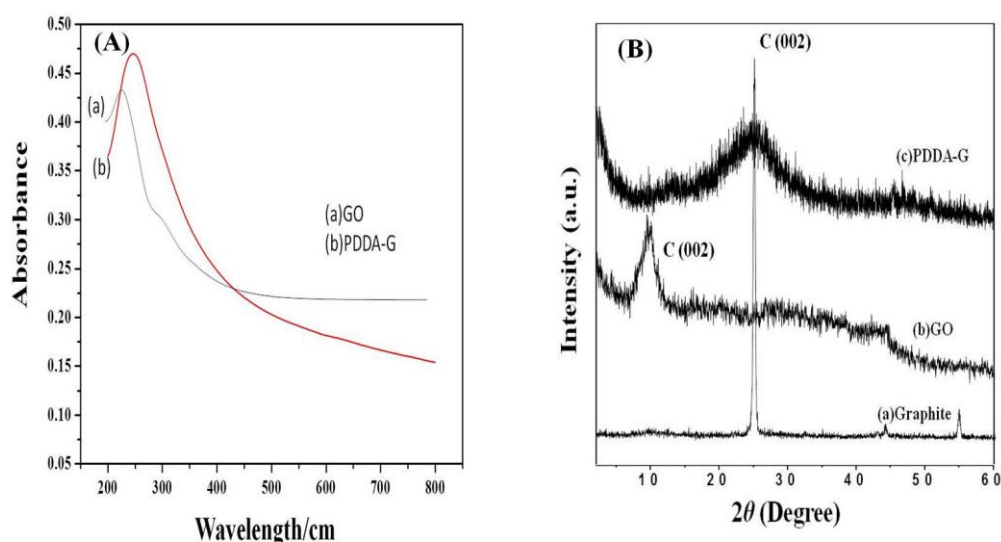


**Figure 2. a** UV spectroscopy of graphene oxide, PDDA-G nanocomposites. **b** XRD patterns of graphite ,graphene oxide, PDDA-G nanocomposites

In order to investigate the the structural information of the graphene, the distance between two layers is a major parameter[19]. The XRD patterns of the Graphite ,GO (curve b) and PDDA-G(curve c) are presented in Fig. 2b. Compared to the graphite powder(curve a) which shows an apparent peak

at  $2\theta=25.9^\circ$  (002), the peak of GO is observed at  $2\theta=9.9^\circ$ (002) (curve b). These results might be stemmed from high level of exfoliation and disordered structure of GO[31]. After microwave reduction by PDDA, a broad peak around  $25.0^\circ$ (curve c) replaces the diffraction peak at  $2\theta=9.9^\circ$ , clearly indicating the disappearance of oxygen functionalities and the completed formation of PDDA-G nanocomposites. Therefore, these as-prepared biofunctional nanocomposites were used for modifying the ITO electrodes.

### 3.2 Characterization of the modified ITO electrodes

To further analyze the electrode modification procedure, the cyclic voltammetry (CV) experiments were used in 5 mM  $K_3[Fe(CN)_6]/K_4[Fe(CN)_6]$  containing 0.1 M KCl. As shown in Fig. 3, a pair of oxidation–reduction peaks at 161 mV and 311 mV were found on the bare ITO (curve a) owing to the reaction of the redox couple  $Fe(CN)_6^{3-}/4^-$ [32]. After the electrode was deposited with PDDA-G (curve b), AuNPs(curve c), successively, the peak current of CVs increased sharply. The reason is the prominent electron transport properties of the aforementioned nanomaterials. Followed by the electrode incubated with capture anti-IL22 (curve d), BSA(curve f), the IL-22(curve e), successively, the peak currents decreased step by step. This might be owing to the inhibition effect of the Immunoconjugates for electron transfer. The results further indicated that the biomoleculars had been immobilized onto successfully and could be used for the proposed immunoassay of IL-22 in the next steps.

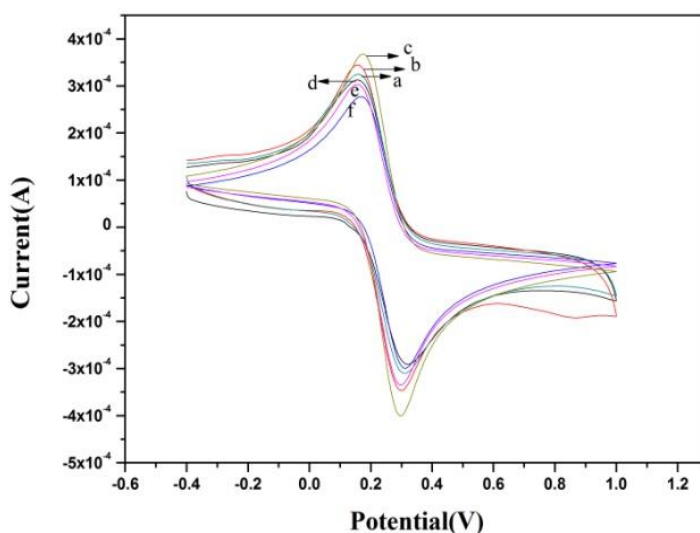


**Figure 3.** CV characterization of the modified modified ITO electrodes in 5 mM  $K_3[Fe(CN)_6]/K_4[Fe(CN)_6]$  solution containing 0.1 M KCl at a scan rate of  $100 \text{ mV s}^{-1}$ : (a)ITO bared, (b) ITO/PDDA-G,(c)ITO/ PDDA-G /AuNPs,(d) ITO/PDDA-G /AuNPs/Antibodies, (e)ITO/ PDDA-G /AuNPs/Antibodies/BSA, (f) ITO/ PDDA-G /AuNPs/Antibodies/BSA/Antigens

### 3.3 Optimization of conditions for electrochemical detection

The analytical performance of the immunosensor was determined mainly by the working concentration of substrates, pH value, incubation time, the proportion of antigen-antibody[33]. After the immunosensor incubation with antigen IL-22 ( $2000 \text{ pg mL}^{-1}$ ), the most appropriate concentrations of OPD and  $\text{H}_2\text{O}_2$  were optimized in Fig. 4a and b. The peak currents trended to reach a peak level when OPD and  $\text{H}_2\text{O}_2$  were at the concentration of 0.2 mM and 0.1 mM, separately. Thus, the optimal OPD (0.2 mM) and  $\text{H}_2\text{O}_2$  (0.1 mM) were used in following experiments, respectively. The pH value of the measurement solution has a great impact on both the activity of the immunoreaction and the electrochemical behavior of the redox mediator. As shown in Fig.4c, the maximum peak current was at the pH of 6.5 in 6 mL PBS (10 mM) containing 0.2 mM OPD and 0.1 mM  $\text{H}_2\text{O}_2$ . Therefore, pH 6.5 was chosen in this work. The effect of incubation time on the electrochemical behavior of IL-22 was investigated with the immunosensor incubation of IL-22 at the concentration of  $2000 \text{ pg mL}^{-1}$ . The peak currents increased with the increasing incubation time range from 15 to 30 min (Fig. 4d), and the determination of IL-22 started to level off occurred at about 30 min. Thus, the optimal incubation time was selected as 30 min in the proposed immunoassay. Besides, the suitable concentrations of capture antibody ( $\text{Ab}_1$ ) and detection antibody ( $\text{Ab}_2$ ) were essential for sandwich immunocomplexes on the surface of the immunosensor[32]. Hence, in order to obtain the maximum formation of the immunoconjugates, the optimal concentrations of  $\text{Ab}_1$  and  $\text{Ab}_2$  were also investigated (Fig. 4e and f)

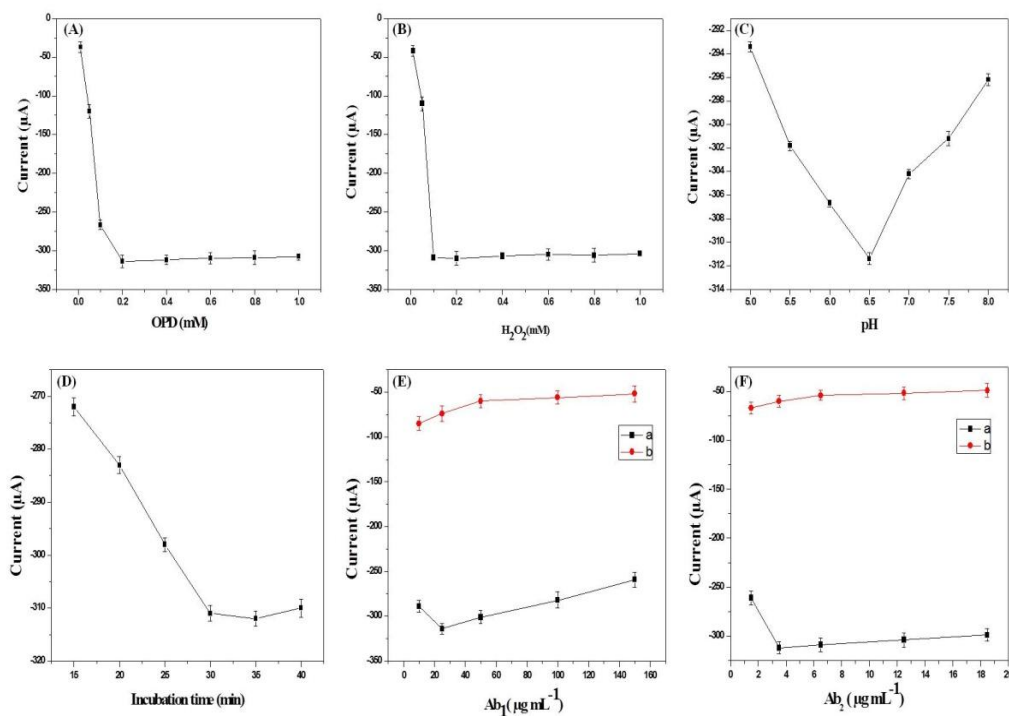


**Figure 4.** Optimization of PDDA-G/AuNPs /ITO **a** using different the concentrations of OPD, **b**  $\text{H}_2\text{O}_2$ , **c** pH, **d** incubation time, **e** DPV responses of Capture antibody ( $\text{Ab}_1$ ), using  $\text{Ab}_2$  at  $3 \text{ } \mu\text{g mL}^{-1}$  and **f** detection antibody ( $\text{Ab}_2$ ), using optimum  $\text{Ab}_1$ . Incubation with IL-22 at  $2000 \text{ pg mL}^{-1}$  and  $0 \text{ pg mL}^{-1}$  (**b**) as control

### 3.4 Specificity and stability of the PDDA-G/AuNPs/ITO immunosensor

The specificity of the immunosensor was tested by incubating with  $1 \text{ ng mL}^{-1}$  of IFN- $\gamma$ , IgG, BSA, or Glucose mixed with a fixed concentration of IL-22 to the immunosensor, respectively (Fig. 5). Followed by the addition, the response of the immunosensor was measured. Generally speaking, the observed selectivity was attributed to the selectivity/specificity of the Ab/Ag reaction and of the non-specific response [13]. Compared with the current response of pure IL-22, these obtained from the interference of IFN- $\gamma$ , IgG, BSA, or Glucose showed small variability. Overall, These results showed that the sandwich devices had a good selectivity. As for the stability of the immunosensor, the nanomaterials modified electrodes were stored at  $4 \text{ }^\circ\text{C}$  for more than four weeks and tested periodically [33]. The variations of DPV responses were less than 5%, indicating the immunosensor possesses a good stability for electrochemical detection. These results depend mostly on the excellent membrane-forming ability of PDDA-G/AuNPs nanocomposites.

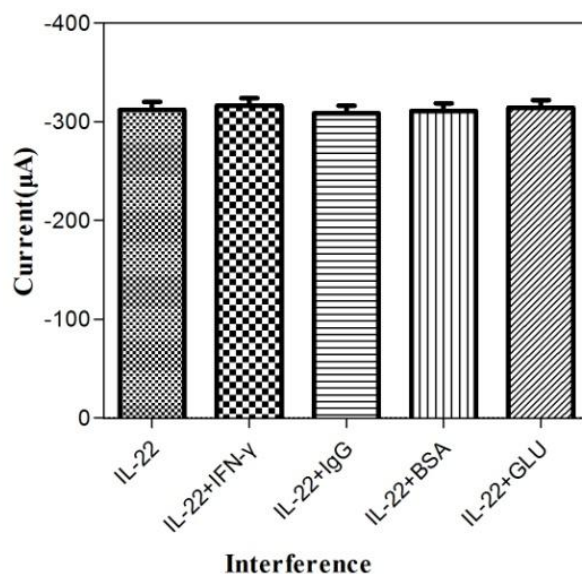


**Figure 5.** Current responses of the immunosensor to  $2000 \text{ pg mL}^{-1}$  IL-22,  $2000 \text{ pg mL}^{-1}$  IL-22 +  $1 \text{ ng mL}^{-1}$  IFN- $\gamma$ ,  $2000 \text{ pg mL}^{-1}$  IL-22 +  $1 \text{ ng mL}^{-1}$  IgG,  $2000 \text{ pg mL}^{-1}$  IL-22 +  $1 \text{ ng mL}^{-1}$  BSA,  $2000 \text{ pg mL}^{-1}$  IL-22 +  $1 \text{ ng mL}^{-1}$  glucose

### 3.5 Analytical performance of the PDDA-G/AuNPs/ITO immunoassay

Under optimal conditions, the immune sensors were incubated with different concentrations of IL-22 standard solutions and detected by DPV measurements. As shown in Fig. 6a, from curve a to curve g, it could be seen that the peak currents increased with the increasing concentrations of the antigens [32]. The calibration plots for the determination of IL-22 were obtained and shown in Fig. 6b. The linear detection relationship (LDR) between the reduction peak currents and the concentration of

analytes was in the ranges of 5 to 5000  $\text{pg mL}^{-1}$  with a correlation coefficient of 0.996 and the limit of detection (LOD) was 0.5  $\text{pg mL}^{-1}$  ( $S/N = 3$ ).

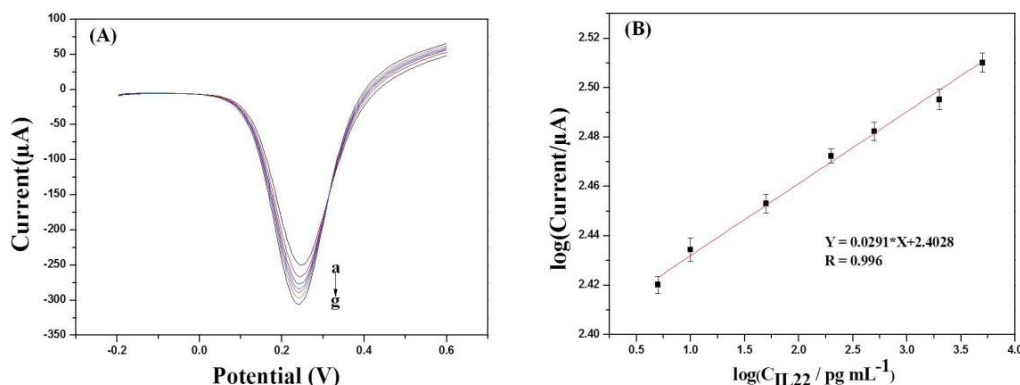


**Figure 6. a** DPV currents of the proposed immunosensor after incubation with IL-22 at different concentrations: 5 (a), 10 (b), 50 (c), 200 (d), 500 (e), 2000 (f) and 5000 (g)  $\text{pg mL}^{-1}$ , respectively. **b** Calibration linear plots for the determination of IL-22 in OPD +  $\text{H}_2\text{O}_2$  + PBS (pH 6.5)

### 3.6 Application in analysis of serum samples

The accuracy of the proposed immunoassay was studied by assaying 5 clinical serum samples. The obtained results were compared with those obtained by enzyme-linked immunosorbent assay (ELISA) as a reference method. The results showed that the proposed method were in good agreement with the reference one, and the relative error between them was less than 5.61% (Table 1). Therefore, the proposed immunosensor could have the potential practical value in the clinical diagnosis of Interleukin-22.

**Table 1.** Assay results of clinical serum samples using the proposed and reference methods

Sample no	Proposed immunosensor ( $\text{pg mL}^{-1}$ )	ELISA ( $\text{pg mL}^{-1}$ )	Relative error (%)
1	47.75	40.28	3.66
2	50.49	53.49	-5.61
3	29.68	30.94	-3.13
4	49.99	47.51	5.21
5	36.31	34.61	4.92

## 4. CONCLUSION

A facile and cheap electrochemical immunoassay based on PDDA-G/AuNPs composites as sensing platform for the detection of cytokine Interleukin-22 was proposed. The DPV currents

increased with the increased antigen concentration due to the increasing signal from the immunoconjugates of HRP as signal tags. The detection process based on PDDA-G and AuNPs with the flexibly controlled size greatly promoted the amount of active sites for capture antibodies load and the electron transfer between the reaction system and the surface of the ITO electrodes. In addition, excellent sensitivity and specificity of the immunosensor were obtained by the sandwich synthesis of Ab<sub>2</sub>-HRP bioconjugates as signal amplification. Therefore, the simple detection strategy demonstrated here offers an promising potential to determination of cytokines and other biomarkers in clinical further applications.

#### ACKNOWLEDGEMENTS

This research was supported by the National science and technology major projects of China ( 2012ZX10004903 ) ,National Natural Science Foundation of China(81473454),the Fundamental Research Funds for Central Universities and Jinan University.

#### References

1. R. Sabat, W. Ouyang and K. Wolk, *Nature Reviews Drug Discovery*, 13 (2014) 21.
2. S. Alonso, K. Pethe, D. G. Russell and G. E. Purdy, *Proc. Natl. Acad. Sci. U. S. A.*, 104 (2007) 6031.
3. M. A. Cobleigh and M. D. Robek, *American Journal Of Pathology*, 182 (2013) 21.
4. H.-F. Pan, X.-P. Li, S. G. Zheng and D.-Q. Ye, *Cytokine Growth Factor Rev.*, 24 (2013) 51.
5. C.-x. Pan, J. Tang, X.-y. Wang, F.-r. Wu, J.-f. Ge and F.-h. Chen, *Inflammation Research*, 63 (2014) 519.
6. H. Fujita, *J. Dermatol. Sci.*, 72 (2013) 3.
7. C. Lim and R. Sayan, *Cytokine Growth Factor Rev.*, 25 (2014) 257.
8. J. M. Leung and P. n. Loke, *International Journal for Parasitology*, 43 (2013) 253.
9. Y. Zhou, M. Wang, Z. Xu, C. Ni, H. Yin and S. Ai, *Biosens. Bioelectron.*, 54 (2014) 244.
10. J. Yang, Y.-G. Nam, S.-K. Lee, C.-S. Kim, Y.-M. Koo, W.-J. Chang and S. Gunasekaran, *Sensors And Actuators B-Chemical*, 203 (2014) 44.
11. T. T. C. Tseng, C.-F. Chang and W.-C. Chan, *Molecules*, 19 (2014) 7341.
12. J. Lin, W. Qu and S. Zhang, *Analytical biochemistry*, 360 (2007) 288.
13. N. S. Ferreira and M. G. Sales, *Biosens Bioelectron*, 53 (2014) 193.
14. C. M. Yu, Z. K. Zhu, L. Wang, Q. H. Wang, N. Bao and H. Y. Gu, *Biosens. Bioelectron.*, 53 (2014) 142.
15. J. H. Lee, B. K. Oh and J. W. Choi, *Biosens Bioelectron*, 49 (2013) 531.
16. V. Dharuman, J. H. Hahn, K. Jayakumar and W. Teng, *Electrochim. Acta*, 114 (2013) 590.
17. J. Yang, J. H. Yu, J. R. Strickler, W. J. Chang and S. Gunasekaran, *Biosens. Bioelectron.*, 47 (2013) 530.
18. D. Li, M. B. Mueller, S. Gilje, R. B. Kaner and G. G. Wallace, *Nature Nanotechnology*, 3 (2008) 101.
19. W. Chen, L. Yan and P. R. Bangal, *Carbon*, 48 (2010) 1146.
20. S. Zhang, Y. Shao, H. Liao, M. H. Engelhard, G. Yin and Y. Lin, *Acs Nano*, 5 (2011) 1785.
21. Z.-G. Le, Z. Liu, Y. Qian and C. Wang, *Appl Surf Sci*, 258 (2012) 5348.
22. G. Wang, L. Chen, Y. Zhu, X. He, G. Xu and X. Zhang, *Biosens. Bioelectron.*, 61 (2014) 410.
23. Y. Yu, Z. Chen, S. He, B. Zhang, X. Li and M. Yao, *Biosens. Bioelectron.*, 52 (2014) 147.
24. L. Cao, Y. Liu, B. Zhang and L. Lu, *Acs Applied Materials & Interfaces*, 2 (2010) 2339.

25. W. Liu, J. Zhang, C. Li, L. Tang, Z. Zhang and M. Yang, *Talanta*, 104 (2013) 204.
26. Y. Song, H. Liu, L. Wan, Y. Wang, H. Hou and L. Wang, *Electroanalysis*, 25 (2013) 1400.
27. R. Wang, J. Di, J. Ma and Z. Ma, *Electrochim. Acta*, 61 (2012) 179.
28. J. Yang, J. R. Strickler and S. Gunasekaran, *Nanoscale*, 4 (2012) 4594.
29. C. Liu, K. Wang, S. Luo, Y. Tang and L. Chen, *Small*, 7 (2011) 1203.
30. S. Liu, J. Q. Tian, L. Wang, Y. L. Luo, W. B. Lu and X. P. Sun, *Biosens. Bioelectron.*, 26 (2011) 4491.
31. J. L. Zhang, H. D. Liu, L. H. Huang, S. Z. Tan, W. J. Mai and X. Cai, *J Solid State Electrochem*, DOI: 10.1007/s10008-014-2595-8 (2014) 1.
32. X. Chen, X. Jia, J. Han, J. Ma and Z. Ma, *Biosens Bioelectron*, 50 (2013) 356.
33. J. Lin, Z. Wei and C. Mao, *Biosens Bioelectron*, 29 (2011) 40.

© 2015 The Authors. Published by ESG ([www.electrochemsci.org](http://www.electrochemsci.org)). This article is an open access article distributed under the terms and conditions of the Creative Commons Attribution license (<http://creativecommons.org/licenses/by/4.0/>).